Degenerate four-wave mixing spectroscopy as a probe of photodissociation dynamics: nascent SH population distributions from the 266 nm photolysis of hydrogen sulfide

ARTICLE · NOVEMBER 1996

4 AUTHORS, INCLUDING:

Thierry Wasserman
Yale University
11 PUBLICATIONS **198** CITATIONS
SEE PROFILE

Thomas Mueller
Bruker Nano Surfaces
36 PUBLICATIONS **461** CITATIONS
SEE PROFILE

15 November 1996

ELSEVIER

Chemical Physics Letters 262 (1996) 329–336

CHEMICAL PHYSICS LETTERS

Degenerate four-wave mixing spectroscopy as a probe of photodissociation dynamics: nascent SH population distributions from the 266 nm photolysis of hydrogen sulfide

Thierry A.W. Wasserman, Angela A. Arias, Thomas Müller, Patrick H. Vaccaro *

Department of Chemistry, Yale University, 225 Prospect Street, New Haven, CT 06511, USA

Received 28 June 1996; in final form 12 September 1996

Abstract

Degenerate four-wave mixing (DFWM) has been used to interrogate the nascent mercapto radicals (SH) emerging from photolysis of bulk-gas H_2S samples at $\lambda_{diss} = 266$ nm. These experiments reveal a 'cold' non-Boltzmann distribution of SH molecules formed exclusively in vibrationless levels of the $X^2\Pi$ ground electronic state, with a non-thermal population of spin–orbit states but no preference for lambda doublet components. Nearly all of the available energy appears as translational motion of the recoiling photofragments. Comparison with previous free-jet studies at $\lambda_{diss} = 193$ nm shows the SH ($v = 0$) rotational distribution to be relatively independent of photolysis wavelength and precursor rotational temperature.

1. Introduction

The field of molecular photodissociation, with its implicit goal of understanding the simplest chemical transformations, has matured to a level of sophistication where theory and experiment provide sufficiently refined information so as to mutually illuminate one another [1]. In part, this enviable situation has been fostered by the myriad of probes that have been developed and successfully employed for the elucidation of photofragmentation processes. While direct spectroscopic interrogation of the parent molecule via either linear absorption or resonance Raman techniques [2] can furnish substantial insight regarding initial stages of the bond rupture event, complimentary information can be derived from investigation of the nascent product species formed upon completion of the photolysis reaction. In the later case, measurements of both scalar (e.g., branching ratios, energy partitioning, and internal state population distribution) and vector (e.g., translational and rotational anisotropies) [3] properties have been found to yield valuable mechanistic details.

The prevalent optical means for interrogating the products of molecular photodissociation are built upon the techniques of laser-induced fluorescence (LIF) spectroscopy. However, when confronted with target species that exhibit short radiative lifetimes or

* Corresponding author.

PII S0009-2614(96)01084-6

poor fluorescence quantum yields, an absorption-based method that retains the high sensitivity and large dynamic range afforded by the background-free response of LIF would be most advantageous. Many of these desirable features can be found in various forms of nonlinear four-wave mixing spectroscopy. This letter demonstrates the feasibility and utility of exploiting the degenerate four-wave mixing (DFWM) scheme as a probe of scalar photofragment properties. In particular, the present work focuses on the photolysis of H_2S molecules at $\lambda_{diss} = 266$ nm (i.e., the extreme red edge of the first H_2S absorption continuum centered at ~ 196 nm), with the population distribution of the nascent mercapto radicals (SH) serving to elucidate the long-time dynamics of the HS–H bond rupture process [4,5]. Analogous two-color transient grating techniques have been developed by Rohlfing, et al. [6,7] and applied to the investigation of NO molecules generated through near-threshold predissociation of NO_2. While all of these studies are conducted in the nanosecond time regime and therefore furnish information on the asymptotic behavior of photodissociation dynamics, Zewail and co-workers [8] recently have shown that similar approaches can be employed for the real-time analysis of a primary photochemical event.

In contrast to the $\tilde{A}$–$\tilde{X}$ transition of water which serves as the prototype for a direct photodissociation process [9], extensive experimental and theoretical studies have demonstrated conclusively that photodissociation through the first absorption continuum of the isoelectronic hydrogen sulfide molecule involves at least two electronically-excited potential energy surfaces [1]. The prevalent model that has emerged from this work suggests an optically-forbidden $^1A_2$ valence state in close proximity to an optically-allowed $^1B_1$ state having substantial Rydberg character [10], with only the former correlating directly to the $H(^2S_{1/2}) + SH(X^2\Pi)$ product asymptote. Extensive ab initio calculations by Schinke and co-workers [11,12] have shown these states to be strongly coupled, possessing two conical intersections along the C_{2v} symmetry axis. Time-dependent wavepacket analyses [12,13] point to a very fast predissociation mechanism where molecules are excited primarily to the bound $^1B_1$ state [i.e., bound with respect to $H(^2S_{1/2}) + SH(X^2\Pi)$] and are transferred rapidly to the dissociative $^1A_2$ surface by a strong non-adiabatic coupling. The small fraction of population remaining in the $^1B_1$ state undergoes a transitory symmetric-stretching motion that gives rise to the diffuse structure observed in the H_2S absorption spectrum [11–14].

The asymptotic product state distributions for H_2S photodissociation have been the subject of several experimental and theoretical investigations. Van Veen and co-workers [15] were the first to exploit time-of-flight (TOF) mass spectrometry to measure the kinetic energy of the recoiling hydrogen atom photofragment and thereby infer the internal state distribution of the simultaneously produced mercapto radicals. For excitation near the peak of the H_2S absorption band ($\lambda_{diss} = 193$ nm), these authors reported the SH fragments to exhibit a bimodal vibrational distribution with most of the molecules formed in $v = 0$ but a secondary population maximum appearing between $v = 3$ and $v = 4$. The fraction of SH molecules generated in vibrationally excited levels was found to increase in proportion to the available energy. Recent extensions of this work by Xie et al. [16] have examined the H atom fragments emerging from H_2S at over a dozen discrete photolysis wavelengths with the latest variants of these studies having sufficient resolution to display unmistakable evidence of SH rotational features [17].

In a pioneering study that preceded the aforementioned work of Van Veen et al., Houston and Hawkins [18,19] exploited LIF spectroscopy as a direct probe of the energy deposited into the mercapto radicals. Photolysis of bulk-gas H_2S samples at $\lambda_{diss} = 193$ nm was found to result in a Boltzmann-like distribution of vibrationless SH molecules characterized by a near-ambient rotational temperature. Experimental difficulties, including insufficient photolysis power and rapid predissociation of the mercapto excited state, hampered detection of vibrationally excited products. Subsequent LIF measurements by Weiner and co-workers [20] resolved many of these obstacles, thereby obtaining rotational distributions for the nascent $SH(v = 1)$ fragments at three photolysis wavelengths ($\lambda_{diss} = 193$ nm, 222 nm, and 248 nm) and for the $SH(v = 1)$ products at $\lambda_{diss} = 193$ nm. These investigations, conducted under both bulk-gas and free-jet expansion conditions, revealed rather 'cold', non-Boltzmann rotational populations that did not exhibit a significant dependence upon the inter-

nal energy of the H_2S species. The present effort represents an extension of such investigations to longer photolysis wavelengths (i.e., $\lambda_{diss} = 266$ nm), with the apparent limitations of LIF detection alleviated through use of the absorption-based DFWM scheme.

Recent years have witnessed a dramatic resurgence of interest in degenerate four-wave mixing [21,22], a coherent process whereby three input beams of identical frequency, ω, interact with a nonlinear medium so as to produce a fourth output or signal beam also having frequency ω. While all incident and generated optical waves are degenerate, they are otherwise distinguishable owing to their directional and/or polarization characteristics. In the absence of strong-field effects (e.g., optical saturation) [23,24], the intensity of the emerging signal, I_s, scales in proportion to the square modulus of the induced third-order polarization, $P_s^{(3)}(t)$, which, in turn, can be expressed as the contraction of the corresponding susceptibility tensor, $\chi^{(3)}(-\omega_s; \omega_f, -\omega_p, \omega_b)$, with the electric field vectors of the impinging waves [25]. In particular, $\chi^{(3)}(-\omega_s; \omega_f, -\omega_p, \omega_b)$ embodies the spectroscopic response of the target molecules (i.e., transition frequencies and decay rates) and exhibits a tremendous increase in magnitude upon resonant excitation of an allowed rovibronic transition.

2. Experimental

For the phase-conjugate DFWM configuration employed in the present studies, the incident and generated optical waves form a plane with their region of mutual intersection defining the sample interaction volume. As shown in Fig. 1, two strong pump beams having electric field vectors E_f (forward-pump) and E_b (backward-pump) are directed through a molecular sample in a coaxial and counterpropagating fashion. A probe beam, with electric vector E_p, crosses the pump fields at a small angle θ. These waves are coupled under the influence of $\chi^{(3)}(-\omega_s; \omega_f, -\omega_p, \omega_b)$ thereby producing a signal field, E_s, which emerges in a direction that precisely retraces the path of the incident probe radiation. A nonlinear response generated in this manner can be shown to satisfy phase-matching or momentum conservation criteria for all angles θ and has the unique property of being a time-reversed or phase-con-

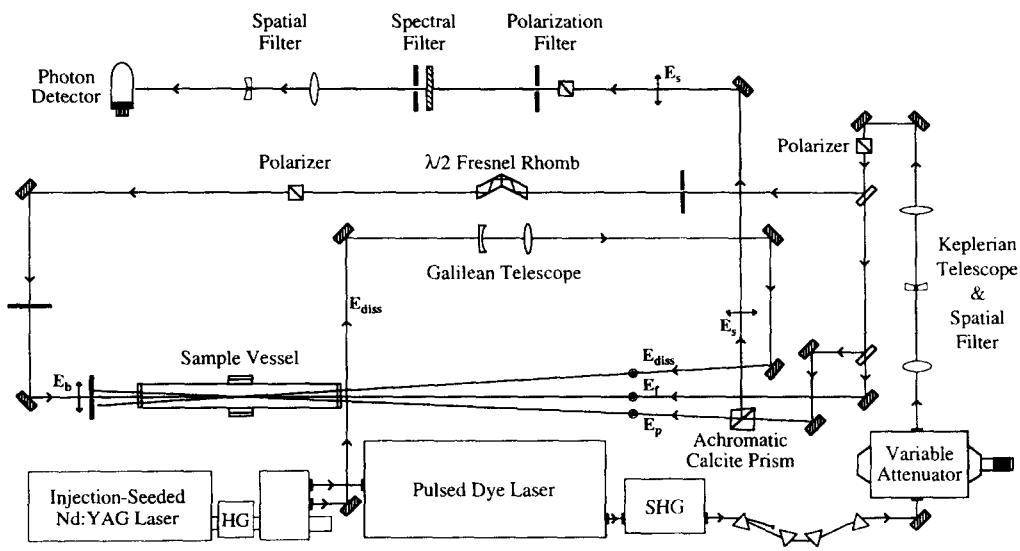

Fig. 1. Schematic diagram of apparatus employed for photodissociation studies. The fourth harmonic of a pulsed Nd:YAG laser (E_{diss}) was used to photolyze a bulk-gas sample of hydrogen sulfide and a counterpropagating (phase-conjugate) implementation of the DFWM scheme (E_f, E_p, E_b, and E_s) was exploited to interrogate the nascent SH photofragments.

jugated replica of the probe beam (i.e., $E_s \propto E_p^*$) [22,23].

The tunable light required for the DFWM detection scheme was obtained by using the second harmonic of a pulsed Nd:YAG laser (Spectra Physics GCR-270-20) to pump a high resolution dye laser (Lambda Physik FL3002E; ~ 0.13 cm^{-1} bandwidth). The fundamental output of this apparatus was frequency doubled by means of a servo-locked KD*P crystal (Inrad Autotracker II) and the resulting ultraviolet radiation was isolated by a set of four Brewster angle prisms.

The frequency-doubled light initially was passed through a variable attenuator which permitted the pulse energy to be varied in a continuous and reproducible fashion. This capability is essential for the saturation studies that must precede any quantitative attempt at DFWM signal interpretation. The ultraviolet output subsequently was directed through a Keplerian telescope where it was spatially filtered and recollimated to a final diameter of 0.3–0.4 cm. A set of achromatic beamsplitters was used to separate the ~ 320 nm radiation into three equivalent beams destined to become the DFWM input waves. In the depicted configuration, the forward-pump (E_f) and probe (E_p) waves have vertical polarization (viz., linear polarization orthogonal to plane of optical table surface) while the backward-pump (E_b) beam has its direction of linear polarization rotated to the horizontal plane ($E_b \perp E_f \| E_p$) by passage through a double (half-wave) Fresnel rhomb. Conservation criteria imposed upon the DFWM interaction [22,23,26] demand that the resulting signal wave (E_s) emerge with a corresponding horizontal polarization (i.e., $E_s \| E_p$), thereby facilitating its discrimination and extraction from the substantially more intense probe radiation.

The counterpropagating pump waves (E_f and E_b) were directed along the central axis of the sample vessel with appropriate delay lines used to ensure their temporal overlap within the DFWM interaction region. The probe beam (E_p) intersected the pump fields under a small angle ($\leq 0.7°$) and ultimately impinged upon an efficient 'black-body' absorber designed to minimize backscattered light. An achromatic prism polarizer was inserted into the probe's optical train to extract the signal photons.

After passing through polarization, spectral, and spatial filters designed to reject stray light, the DFWM signal beam impinged upon the photocathode of an uncooled photomultiplier tube. The resulting photocurrent was preamplified and directed to a CAMAC based gated-integrator system that enabled the signal intensity to be measured as a function of laser wavelength. Absolute and relative frequency calibrations, as well as the incident pulse energy, were recorded simultaneously. Pulse-to-pulse fluctuations in the DFWM signal amplitude were minimized through use of an active normalization procedure. A microcomputer-based software package coordinated scanning of dye laser frequency and acquisition of experimental data sets.

The 266 nm photolysis light was generated by directing a portion of the Nd:YAG second harmonic through an external KD*P frequency doubler. The resulting ultraviolet radiation was isolated by a series of dichroic beamsplitters, weakly focused by means of a Galilean telescope (~ 1 cm spot diameter), and directed into the sample vessel at a small crossing angle that gave appreciable overlap with the four-wave mixing interaction volume. An optical delay line was installed to ensure that the photofragmentation pulse (E_{diss}) arrived at the product detection region ~ 7 ns prior to the DFWM interrogation pulses. Measurements performed with a second, independently-triggerable photolysis source confirmed the nascent character of the SH internal state distributions acquired under such conditions. Typical 266 nm energies were 50–70 mJ/pulse and the energy of each DFWM beam was attenuated to ≤ 250 nJ/pulse so as to minimize complications arising from optical saturation effects. For the scalar results reported in this Letter, the linear polarization for the photolysis light was held fixed in the vertical direction.

The sample cell was constructed from a one meter long section of glass tubing with high quality fused silica windows mounted upon o-ring seals at both ends. A diffusion pumped vacuum system enabled this vessel to be evacuated to base pressures of $< 10^{-5}$ Torr while manual adjustment of the inlet and outlet valves permitted a continuous flow of hydrogen sulfide gas (Matheson; 99.5% stated purity) to be established. The steady state pressure of H_2S precursor was monitored by means of a capacitance manometer and typically maintained in the 500 mTorr range.

3. Results and discussion

The feasibility of exploiting four-wave mixing as a probe of nascent photofragments is demonstrated by Fig. 2 which presents a portion of the SH $A^2\Sigma^+$–$X^2\Pi$ (0,0) band recorded subsequent to the 266 nm photolysis of a bulk-gas hydrogen sulfide sample. The small photodissociation cross-section of H_2S at this wavelength ($\sigma_{266} \approx 6 \times 10^{-22}$ cm^2) [27], coupled with the sub-nanosecond predissociation lifetimes reported for the $A^2\Sigma^+$ state of the mercapto radical [28], encumbers the implementation and interpretation of conventional LIF techniques. These factors also affect the strength of recorded DFWM spectral features, with the concomitant use of unfocused, low-power incident beams necessitating relatively high sample pressures for the acquisition of high quality data sets. The 'collision-free' nature of these experimental conditions was confirmed by performing a series of measurements with varying time delays between the optical pulses responsible for precursor photolysis and product interrogation. Taking into account the low photofragmentation efficiency [27] of H_2S at $\lambda_{diss} = 266$ nm, unsaturated spectra such as that depicted in Fig. 2 translate into an estimated detection limit of $< 10^{11}$ molecules/cm^3/quantum state (NB., much better sensitivities can be obtained under conditions of optical saturation). The one-photon character of the photolysis process was assessed by examining the influence of 266 nm power upon the yield ofSH photoproducts. The DFWM response was found to scale in proportion to the square of the applied 266 nm pulse energy, a result in keeping with the expected quadratic dependence of four-wave mixing intensity upon sample number density [21–23].

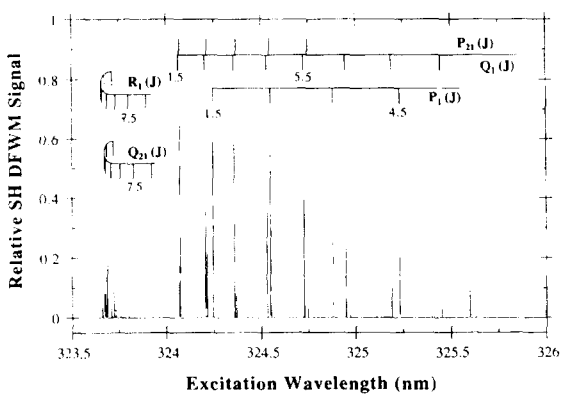

Fig. 2. DFWM spectrum of nascent photoproducts. The phase-conjugate DFWM scheme was used to interrogate the nascent mercapto radicals generated in the 266 nm photolysis of H_2S. The depicted spectrum shows a portion of the SH $A^2\Sigma^+$-$X^2\Pi$ (0,0) band with superimposed branch assignments derived from the spectroscopic work of Ramsay, et al. [35]. Each peak corresponds to the formation of product molecules in a specific rotational level of the vibrationless ground electronic state.

Given the HS–H bond dissociation energy of 3.91 ± 0.2 eV [29], the 266 nm photolysis of a room temperature H_2S sample will result in roughly 0.8 eV of excess energy to be apportioned among accessible product channels. This quantity of energy, although insufficient to create electronically-excited mercapto radicals, can lead to the formation of SH photoproducts exhibiting moderate rovibrational excitation, with energy constraints suggesting the possible population of vibrational states up to $v = 2$ and of vibrationless rotational levels as high as $J = 25.5$. The unsaturated $N^2|\mu|^8$ dependence [22] of DFWM signal strength on number density (N) and transition dipole moment (μ) precludes extraction of internal state distributions from a cursory inspection of Fig. 2, however, qualitative features can readily be discerned. In particular, nascent SH molecules are found to reside only in vibrationless levels of the $X^2\Pi_{3/2}$ and $X^2\Pi_{1/2}$ spin–orbit doublet, with rotational states beyond $J = 10.5$ containing negligible population. This suggests that the major fraction of available energy ($> 90\%$) appears as relative translational motion of the departing fragments, a result in keeping with those obtained in previous TOF [15,16,30] and LIF [18–20] measurements.

Reduction of the DFWM data to relative populations for SH internal quantum states was based upon a weak-field perturbative treatment [25,31,32] in which the integrated areas of individual spectral peaks were normalized by the square modulus of the third-order signal polarization, $\boldsymbol{P}_s^{(3)}(t)$, induced by the impinging optical waves. In particular, calculation of $\boldsymbol{P}_s^{(3)}(t)$ entailed direct evaluation of the corresponding nonlinear susceptibility, $\chi^{(3)}(-\omega_s; \omega_f, -\omega_p, \omega_b)$, for each SH rovibronic transition (i.e., including effects associated with incident light polarizations, excited state predissociation, and finite laser excitation bandwidth), followed by numerical integration of the resulting expression over model distri-

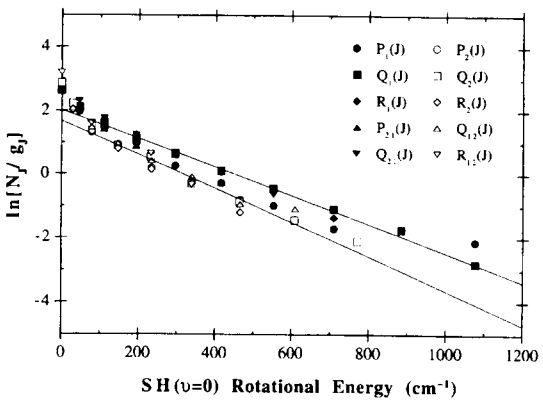

Fig. 3. Boltzmann plot for vibrationless SH radicals formed from 266 nm photolysis of H_2S. The logarithm of relative rotational population (N_J) normalized by rotational degeneracy (g_J) is plotted as a function of rotational energy for ground levels corresponding to the various branches of the SH $A^2\Sigma^+ - X^2\Pi$ (0,0) band. Effective rotational temperatures of 320 ± 20 K and 270 ± 25 K (1σ uncertainties) are obtain for the vibrationless $X^2\Pi_{3/2}$ and $X^2\Pi_{1/2}$ states, respectively.

butions of photofragment velocities. Since comparison of main and satellite branch intensities [32] revealed that the effective quadrupolar alignment moment [33], $A_0^{(2)}(J)$, of the mercapto radicals was negligibly small, no correction was made for rotational anisotropy of the photoproducts. A detailed analysis of this and other vector correlation measurements in the context of DFWM spectroscopy is relegated to a future publication [34].

The distribution of nascent SH photofragments among their vibrationless rotational levels is summarized by the Boltzmann plot of Fig. 3. While the depicted data sets clearly deviate from the strictly linear relationship that would characterize a thermally-equilibrated process, the higher-lying members of the $Q_1(J)$ and $Q_2(J)$ branches lead to effective rotational temperatures of 320 ± 20 K and 270 ± 25 K, respectively, for the $^2\Pi_{3/2}$ and $^2\Pi_{1/2}$ spin–orbit manifolds. These results corroborate the significant partitioning of available energy into translational degrees of freedom and reinforce the 'cold' nature of rotational distributions reported in previous LIF studies [18–20] conducted at photolysis wavelengths in closer proximity to the H_2S absorption maximum. The unrelaxed mercapto radicals exhibit a propensity for the lower spin–orbit state (viz., $^2\Pi_{3/2}$), with the $^2\Pi_{3/2}/^2\Pi_{1/2}$ population ratio of 2.10 ± 0.15 deviating from that expected for a thermal distribution of 'cold' SH molecules characterized by a $X^2\Pi$ spin–orbit constant [35] of -376.9 cm^{-1}. The SH lambda doublet components were found to have a J-averaged occupation ratio of $\Pi(A')/\Pi(A'') = 1.06 \pm 0.07$ indicating no significant preference for a particular orientation of the electronic angular momentum during the photofragmentation event.

The $SH(X^2\Pi_{3/2};\ v=0)$ rotational distribution measured (with DFWM) for the 266 nm photodissociation of H_2S under ambient (~ 300 K) bulk-gas conditions is presented in Fig. 4 along with analogous results obtained (with LIF) from 193 nm experiments [20] performed on jet-cooled (~ 10 K) samples. Despite substantial differences in the wavelength of photolysis (viz., available energy) and initial degree of precursor excitation (viz., H_2S rovibrational temperature), these distinct data sets exhibit distributions that are near-identical in shape and extent. This observation can be rationalized through the 'rotational Franck–Condon principle' [1] which describes the invariant, Gaussian-like nature of such distributions as a manifestation of the vibrational wavefunction for ground state H_2S bending motion being projected directly onto the individual eigenfunctions of the free SH rotor. In particular, this interpretation implies an absence of anisotropic forces

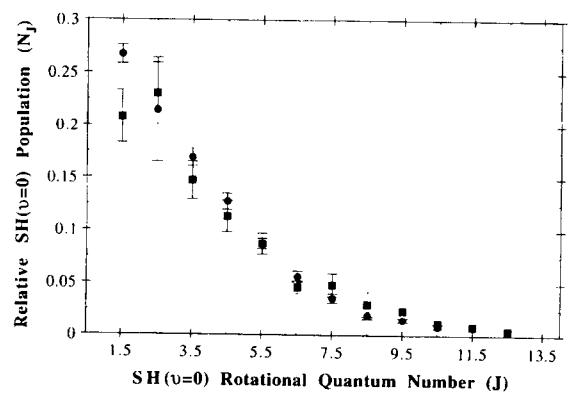

Fig. 4. Comparison of vibrationless SH population distributions. $SH(X^2\Pi_{3/2};\ v=0)$ rotational distributions are compared for measurements performed under two distinct sets of experimental conditions: (●) 266 nm photolysis under ambient (~ 300 K) bulk-gas conditions via DFWM and (■) 193 nm photolysis under jet-cooled (~ 10 K) conditions via LIF [20].

in the dissociative excited state(s) of hydrogen sulfide, with negligible influence of parent rotation on the overall dynamics of photodissociation.

4. Summary and conclusions

The nonlinear optical technique of degenerate four-wave mixing has been used to probe the unrelaxed mercapto radicals produced upon photolysis of H_2S molecules at the extreme red-edge of their first absorption continuum (i.e., $\lambda_{diss} = 266$ nm). Detailed analysis of DFWM spectra revealed a non-Boltzmann rotational distribution of nascent SH molecules created exclusively within the vibrationless levels of the $X^2\Pi$ manifold, with a non-thermal preference for the lower-lying spin–orbit component but no significant disparity in population between the members of a lambda doublet. Effective rotational temperatures derived from high-J lines are 'cold' and remarkably similar to those obtained in previous studies [20] performed at $\lambda_{diss} = 193$ nm. These results suggest that more than 90% of the available energy is channeled into translational motion of the recoiling photofragments.

As demonstrated by the work presented above, DFWM spectroscopy provides a viable method for interrogating the unrelaxed products of a primary photochemical event. While the underlying nature of the four-wave mixing interaction precludes attainment of idealized 'single particle' detection limits, the unique capabilities afforded by such absorption-based schemes can prove to be advantageous for studies of molecular structure and dynamics [21,22]. In addition to the scalar photodissociation properties examined in this letter, ongoing efforts in our laboratory have successfully exploited the polarization specificity and velocity discrimination inherent to sub-Doppler DFWM implementations as a means of elucidating the rotational [32] and translational [34] anisotropy of nascent photofragments.

Acknowledgements

This work was performed under the auspices of grants provided by the United States National Science Foundation, Directorate of Experimental Physical Chemistry. The authors wish to thank Dr. B.R. Johnson (Rice Quantum Institute) and Prof. W.A. Chupka (Yale University) for useful discussions. P.H.V. gratefully acknowledges the Camille and Henry Dreyfus Foundation for a Camille Dreyfus Teacher–Scholar Award and The David and Lucile Packard Foundation for support through a Packard Fellowship for Science and Engineering.

References

[1] R. Schinke, Photodissociation Dynamics: Spectroscopy and Fragmentation of Small Polyatomic Molecules, (Cambridge Univ. Press, Cambridge, 1993).
[2] B.R. Johnson, C. Kittrell, P.B. Kelly, and J.L. Kinsey, J. Phys. Chem. 100 (1996) 7743.
[3] G.E. Hall and P.L. Houston, Ann. Rev. Phys. Chem. 40 (1989) 375.
[4] T.A.W. Wasserman, A.A. Arias, T. Müller, and P.H. Vaccaro, in: Proceedings of 50th International Conference on Molecular Spectroscopy, Ohio State University, Columbus, Ohio (1995).
[5] T.A.W. Wasserman, A.A. Arias, T. Müller, and P.H. Vaccaro, in: Proceedings of 1995 Conference on the Dynamics of the Molecular Collisions, Asilomar, California (1995).
[6] T.J. Butenhoff and E.A. Rohlfing, J. Chem. Phys. 98 (1993) 5460.
[7] T.J. Butenhoff and E.A. Rohlfing, J. Chem. Phys. 98 (1993) 5469.
[8] M. Motzkus, S. Pedersen, and A.H. Zewail, J. Phys. Chem. 100 (1996) 5620.
[9] V. Engel, V. Staemmler, R.L. Vander Wal, F.F. Crim, R.J. Sension, B. Hudson, P. Andresen, S. Hennig, K. Weide, and R. Schinke, J. Phys. Chem. 96 (1992) 3201.
[10] K.O. Lantz and V. Vaida, Chem. Phys. Lett. 215 (1993) 329.
[11] K. Weide, V. Staemmler, and R. Schinke, J. Chem. Phys. 93 (1990) 861.
[12] B. Heumann, K. Weide, R. Düren, and R. Schinke, J. Chem. Phys. 98 (1993) 5508.
[13] B. Heumann and R. Schinke, J. Chem. Phys. 101 (1994) 7488.
[14] K. Weide, K. Kuhl, and R. Schinke, J. Chem. Phys. 91 (1989) 3999.
[15] G.N.A. Van Veen, K.A. Mohamed, T. Baller, and A.E. De Vries, Chem. Phys. 74 (1983) 261.
[16] X. Xie, L. Schneider, H. Wallmeier, R. Boettner, K.H. Welge, and M.N.R. Ashfold, J. Chem. Phys. 92 (1990) 1608.
[17] G.P. Morley, I.R. Lambert, D.H. Mordaunt, S.H.S. Wilson, M.N.R. Ashfold, R.N. Dixon, and C.M. Western, J. Chem. Soc. Faraday Trans. 89 (1993) 3865.
[18] W.G. Hawkins and P.L. Houston, J. Chem. Phys. 76 (1982) 729.
[19] W.G. Hawkins and P.L. Houston, J. Chem. Phys. 73 (1980) 297.

[20] B.R. Weiner, H.B. Levene, J.J. Valentini, and A.P. Baronavski, J. Chem. Phys. 90 (1989) 1403.
[21] R.L. Farrow and D.J. Rakestraw, Science 257 (1992) 1894.
[22] P.H. Vaccaro, in: Molecular Dynamics and Spectroscopy by Stimulated Emission Pumping, eds. H.-L. Dai and R.W. Field (World Scientific Publishing, Singapore, 1995), p. 1.
[23] R.L. Abrams, J.F. Lam, R.C. Lind, D.G. Steel, and P.F. Liao, in: Optical Phase Conjugation, ed. R.A. Fisher (Academic Press, San Diego, 1983), p. 211.
[24] S. Williams, R.N. Zare, and L.A. Rahn, J. Chem. Phys. 101 (1994) 1093.
[25] P.N. Butcher and D. Cotter, The Elements of Nonlinear Optics, (Cambridge Univ. Press, Cambridge, 1990).
[26] J.F. Reintjes, Nonlinear Optical Parametric Processes in Liquids and Gases Molecules, (Academic Press, New York, 1984).
[27] J. Zoval, D. Imre, P. Ashjian, and V.A. Apkarian, Chem. Phys. Lett. 197 (1992) 549.
[28] W. Ubachs and J.J. ter Meulen, J. Chem. Phys. 92 (1990) 2121.
[29] H. Okabe, Photochemistry of Small Molecules, (John Wiley and Sons, New York, 1978).
[30] Z. Xu, B. Koplitz, and C. Wittig, J. Chem. Phys. 87 (1987) 1062.
[31] S. Williams, R.N. Zare, and L.A. Rahn, J. Chem. Phys. 101 (1994) 1072.
[32] T.A.W. Wasserman, A.A. Arias, S.A. Kandel, D. Hsu, and P.H. Vaccaro, SPIE 2548 (1995) 220.
[33] R.N. Zare, Angular Momentum, (John Wiley and Sons, New York, 1988).
[34] T.A.W. Wasserman, B.R. Johnson, and P.H. Vaccaro, work in progress.
[35] D.A. Ramsay, J. Chem. Phys. 20 (1952) 1920.